River Research and Applications

WILEY

RESEARCH ARTICLE OPEN ACCESS

Dam It, I'm Stranded: Evaluating Fish Stranding Downstream of Two Hydropeaking Dams in Northern Ontario

Raegan Davis[1] | Steven J. Cooke[1] | Karen E. Smokorowski[2]

[1]Department of Biology, Fish Ecology and Conservation Physiology Laboratory, Carleton University, Ottawa, Ontario, Canada | [2]Ecosystem Sciences Division, Fisheries and Oceans Canada, Sault Sainte Marie, Ontario, Canada

Correspondence: Raegan Davis (raegandavis@cmail.carleton.ca)

Received: 22 October 2025 | **Revised:** 3 January 2026 | **Accepted:** 8 January 2026

Keywords: fish stranding | hydropeaking | mitigation | remote photography

ABSTRACT

Globally, there has been an increase in the development and use of hydropower to produce energy. Hydropeaking is an operating regime that is used to meet real-time energy demands; however, daily fluctuations in flows may result in fish becoming stranded. Understanding physical and operational factors that contribute to fish stranding will aid in the creation of mitigation strategies to prevent fish stranding occurrences. Here we investigated factors that drive fish stranding. To do so, we deployed cameras downstream of two hydropeaking generating stations in northern Ontario, Canada, from June to October in 2023 and 2024, to remotely capture occurrences of fish stranding. We observed significantly higher fish stranding densities (fish m^{-2}) on the Michipicoten River compared to the Magpie River. Stranded fish were difficult to identify to species (from the camera images) but in general, fish were small-bodied, likely representing early life stages (e.g., juveniles). The probability of fish stranding was highest in the early spring and increased with both finer substrate types and slower horizontal ramping rates (cm h^{-1}). The observed differences in fish stranding densities between the two rivers are likely due to physical features such as the absence of morphological microstructures, larger substrate types, and the presence of a plunge pool (at one site). The plunge pool likely dampened the change in discharge from the dam, which subsequently decreased the vertical ramping rate (cm h^{-1}) downstream. The model we generated will allow for comparison with other hydropeaking systems globally to better understand if factors driving fish stranding are common among rivers to help identify potential mitigation strategies to minimize stranding.

1 | Introduction

The energy sector is currently one of the largest contributors of atmospheric greenhouse gas emissions (Bauer et al. 2017; IPCC 2023). To reduce such emissions many countries have made commitments (e.g., Paris Agreement 2015, Canada's 2030 Emissions Reduction Plan) embracing renewable and low-carbon energy resources such as hydropower, solar, and wind to meet growing energy demands during the phase-out of coal-powered electricity. Of the existing renewable energy options, hydropower plays the largest role, generating approximately 78% of renewable electricity globally (Berga 2016). To respond to real-time energy demands, a hydroelectric generating station (GS) may employ a hydropeaking flow regime. Peaking events occur when the dam changes from minimum discharge to maximum discharge and then back to minimum discharge, which can occur daily or sub-daily depending on market energy demands and operational capacities (Li and Pasternack 2021; Smokorowski 2022). Consequently, these peaking events can have negative impacts on fish (Nagrodski et al. 2012; Young et al. 2011), invertebrates (Kjærstad et al. 2018; Timusk et al. 2016), riparian

plants (Bejarano et al. 2018; Butterfield and Palmquist 2025), and sediment transport (Béjar et al. 2018; Nguyen et al. 2025) on the river reach downstream from a GS.

A potential ecological impact of hydropeaking is fish stranding, which occurs when fish become stranded on dry substrate or in pools disconnected from the main channel after a peaking event (Glowa, Watkinson, et al. 2023; Irvine et al. 2015; Larrieu et al. 2021; Nagrodski et al. 2012; Young et al. 2011). Fish stranding can result in mortality through desiccation, asphyxiation, and predation; however, if fish are isolated in pools they may survive if the pool maintains adequate environmental conditions and becomes reconnected during a subsequent peaking event (Glowa, Watkinson, et al. 2023; Saltveit et al. 2001; Young et al. 2011). All life stages of fish can be negatively impacted by hydropeaking operations. The reduced swimming capacity and habitat preferences for areas that frequently become dewatered during peaking events increase the stranding risk of juvenile and small-bodied fishes (Armstrong et al. 2003; Eppehimer et al. 2021; Haas et al. 2016; Insulaire et al. 2024; Irvine et al. 2015; Saltveit et al. 2001). As fish increase in size, their habitat preferences often change and their swimming capabilities improve, which decreases their vulnerability to stranding (Hunter 1992; Young et al. 2011). Over time, repeated peaking events can have negative consequences on fish populations and communities, such as lowering the abundance of juvenile and small-bodied fishes (Enders et al. 2017), depleting populations (Hayes et al. 2024), and the mortality of millions of fish each year (Glowa, Kneale, et al. 2023).

The operational regime of the hydropeaking GS can influence the likelihood of fish stranding. The down-ramping rate, which is the rate of change in discharge released from the dam from maximum to minimum, can play a critical role in fish stranding likelihood (Nagrodski et al. 2012; Moreira et al. 2019; Young et al. 2011). In general, slower down-ramping rates reduce fish stranding occurrences as fish have more time to respond to changes in flow (Moreira et al. 2019). The length of time that a site remains wetted also influences fish stranding probability, with Irvine et al. (2015) observing a positive relationship between fish stranding and time that a site remained wet.

Physical characteristics of the river can influence the likelihood of fish stranding on hydropeaking rivers. River morphology features, such as the presence of side channels and gravel bars, increase fish stranding occurrences (Bradford 1997; Hayes et al. 2023). Repeated changes in discharge from the dam often result in the formation of morphological microstructures (e.g., scour pools, potholes, and alluvial puddles) on finer substrates which are known hotspots of fish stranding (Insulaire et al. 2024). Fish stranding is also influenced by the slope of the riverbank, with steeper slopes (> 6%) reducing fish stranding occurrences compared to gentler slopes (< 4%; Bradford et al. 1995; Führer et al. 2022; Hunter 1992). The horizontal ramping rate, which is related to the slope of the riverbank, has been identified as a highly relevant contributor to fish stranding, with faster horizontal ramping rates increasing the likelihood of fish stranding (Hauer et al. 2017; Le Coarer et al. 2023). Substrate size can also influence fish stranding, although differences exist within the literature (Glowa, Watkinson, et al. 2023; Hunter 1992). Glowa, Watkinson, et al. (2023) reported higher occurrences of fish stranding on finer substrates, whereas Hunter (1992) reported that fish stranding was more likely on large substrates.

The aim of this study was to further explore the impacts of hydropeaking on fish stranding to identify potential mitigative strategies. Given that fish stranding is a concern on regulated rivers, we selected two hydropeaking rivers in northern Ontario, Canada with different operational and physical characteristics. Here, we deployed trail cameras on both rivers below their GS to document stranding using previously developed methods (Glowa, Watkinson, et al. 2023). Using the same methodology as Glowa, Watkinson, et al. (2023) extends the ability to learn from this novel method on different rivers while enabling the comparison of model results, helping to contribute to the broader understanding of what factors drive fish to strand on hydropeaking rivers. The specific objectives of this study were to (1) quantify fish stranding density (fish m^{-2}) occurring downstream of two hydropeaking generating stations; (2) compare fish stranding densities (fish m^{-2}) obtained from two different assessment methodologies (e.g., remote photography and quadrat sampling); (3) determine fish species and sizes (mm) that are susceptible to stranding on hydropeaking rivers; (4) determine what factors (e.g., wetted history [min], horizontal ramping rate [cm h^{-1}], calendar day [day], substrate [mm], and fish density [fish m^{-2}]) drive fish stranding on hydropeaking rivers; and (5) determine if factors that drive fish stranding are the same between rivers with different hydropeaking regimes.

2 | Methods

2.1 | Study Sites

Two hydroelectric generating stations that operate with hydropeaking regimes located near the town of Wawa, Ontario (47.9888°, −84.7741°) were selected for this study. The first hydroelectric GS is Scott Falls (47.9103°, −84.7449°), located on the Michipicoten River (MR), commissioned in 1952 with a 22.5 MW generation capacity, a maximum turbine flow of 100 $m^3 s^{-1}$ and a minimum flow of 17 $m^3 s^{-1}$ (Figure 1a). From April 15 to June 15, Scott Falls GS operates with an increased minimum flow of 26.3 $m^3 s^{-1}$ to support spawning of rainbow trout (*Oncorhynchus mykiss*). Scott Falls GS is the most downstream of four operating hydroelectric stations on the MR, after which the river flows directly into eastern Lake Superior. The study reach was 3 km in length, beginning approximately 250 m downstream from Scott Falls GS. The river reach on the MR susceptible to changing flows from the GS is approximately 10.5 km (linear distance of river measured by Google Earth Pro v.7.3.6) with vulnerability to fish stranding decreasing at the end of our study reach due to habitat changes that attenuate flow changes (e.g., steep slopes that lack gravel bars). Being open to Lake Superior, fish are free to move into the river throughout the year, and many species are known to spawn in the river reach downstream from Scott Falls GS (e.g., rainbow trout and lake sturgeon [*Acipenser fulvenscens*] spawning in the early spring while lake trout [*Salvelinus*

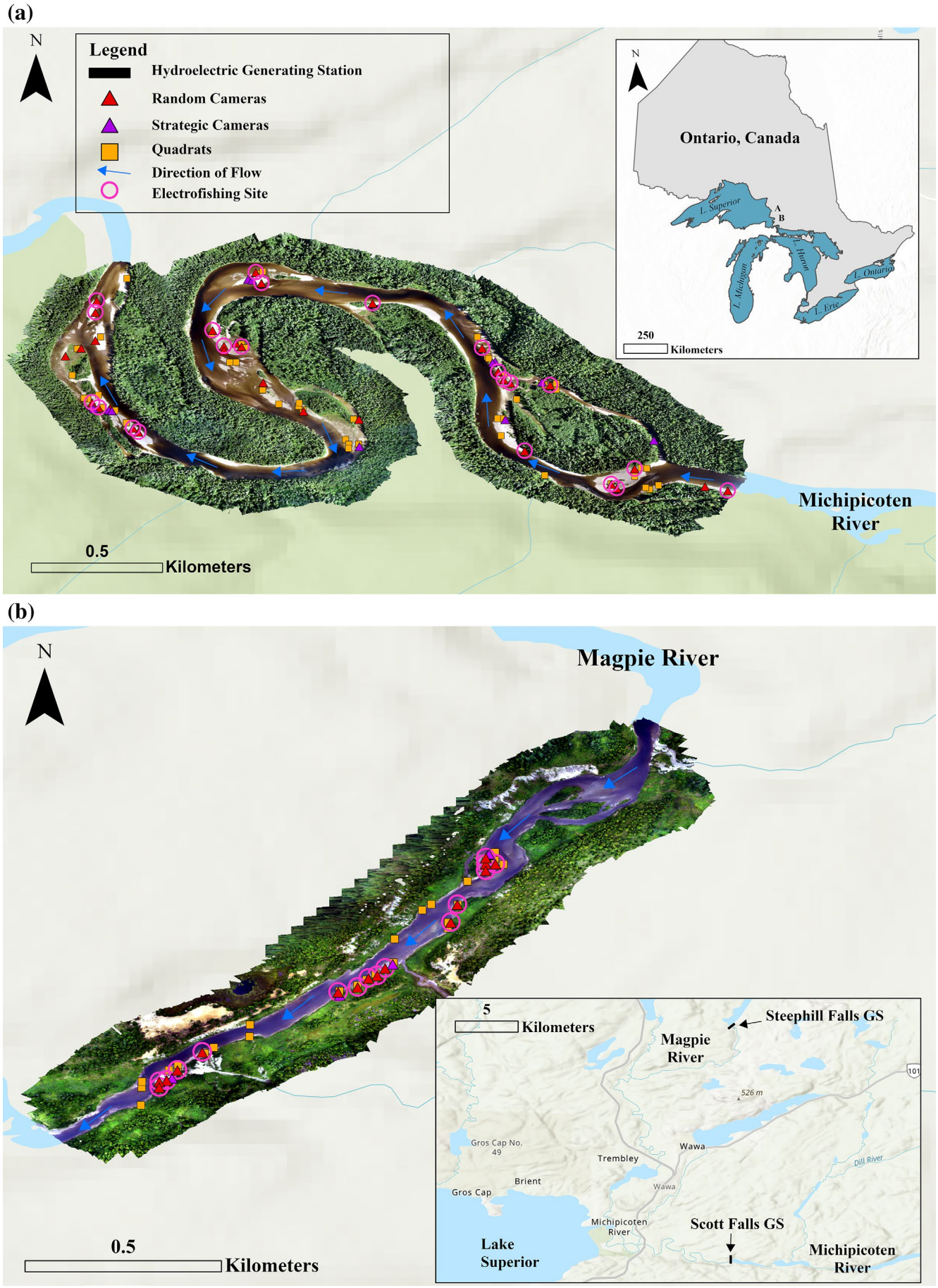

FIGURE 1 | Legend on next page.

FIGURE 1 | Map showing the location of the (a) Michipicoten River, and (b) Magpie River Wawa, Ontario, Canada. Camera locations for both study years are shown with red triangles (random) and purple triangles (strategic). Quadrat locations for both study years are shown with orange squares. Electrofishing sites are shown with pink circles. Locations of study hydroelectric generating stations are identified with black bar. [Color figure can be viewed at wileyonlinelibrary.com]

namaycush], chinook salmon [*Oncorhynchus tshawytscha*], coho salmon [*Oncorhynchus kisutch*], and pink salmon [*Oncorhynchus gorbuscha*] spawn in the late summer into the fall). The second hydroelectric GS is Steephill Falls (48.0771°, −84.7393°), located on the Magpie River (MPR), which was commissioned in 1989 with a 16 MW generation capacity, a maximum turbine flow of 45 $m^3 s^{-1}$ and a minimum flow of 7.5 $m^3 s^{-1}$ (Figure 1b). The study reach was 1 km in length, beginning approximately 2 km downstream from Steephill Falls GS. The river reach on the MPR susceptible to changing flows is approximately 12 km (linear distance of river measured by Google Earth Pro v.7.3.6) with vulnerability to fish stranding decreasing at the downstream end of our study reach due to inflows from groundwater and tributaries that attenuate changes in flow. The study reach of the MPR is a closed system with two downstream hydroelectric generating stations that prevent fish migrations from Lake Superior.

2.2 | Photography

To identify locations with potential for fish stranding, photogrammetry mapping was conducted in August of 2022 on each river which produced a digital elevation model (DEM). Locations susceptible to fish stranding were identified as sites that became both inundated and dry throughout the course of a peaking event. Then a 15 m-by-15 m grid was overlayed on the DEM of the river reaches in R (R Core Team 2023), using the exactextractr (v0.7.2; Batson 2021), rgeo (v0.5-8; Bivand and Rundel 2021), and rgal (v1.5-27; Bivand et al. 2021) packages. Subsequently, 8 random sites were selected for each river in 2023, and for the MPR in 2024. Because the reach on the MR was three times longer than the MPR, in 2024, a stratified random sampling approach was taken to balance the relative spatial coverage on each river. To facilitate this, the original 2023 study reach on the MR was divided into three approximately 1 km reaches: reach 1 (47.9099°, −84.7576°), reach 2 (47.9581°, −85.7323°), and reach 3 (47.9534°, −84.7418°). Eight locations were randomly selected in each reach, resulting in 24 total random sites in 2024. Recognizing that fish stranding is reported to be patchy, strategic site locations were also selected with features thought to be conducive to fish stranding (e.g., potholes, gentle slopes, and fine substrate types). For both rivers in 2023, and for the MPR in 2024, 3 strategic sites were selected. On the MR in 2024, 3 strategic sites were selected for each study reach totaling 9 strategic sites.

Remote photography methodology (Glowa, Watkinson, et al. 2023) was completed at each selected site on both rivers from June to October in 2023 and 2024 (Figure 2). Time lapse cameras (Boly trail camera, model 2G2060-D, SG562-C, SG2060T, Victoriaville, QC, Canada) were used to capture occurrences of fish stranding by attaching them to custom-made camera mounts that pointed downwards towards the river substrate, with a mean height of 3.67 m and photographed area of $7.37 \pm 0.82\ m^2$ (Figure 3; see Glowa, Watkinson, et al. 2023 for full description of camera mounts). Cameras were programmed to take a photograph every 30 min to capture changing water levels during peaking events from the GS. Camera mounts were visited monthly for general maintenance (e.g., battery swaps, clearing of spider webs, and tightening of ropes) and to exchange SD cards.

2.3 | Quadrats

To compare methodologies, quadrat sampling was conducted during monthly visits to the rivers when the GS was peaking. A quadrat that was 2.55 m by 2.55 m, with a sampling area of 6.50 m^2 was used to approximate the area captured by each camera image. Twelve sites were randomly selected each month using a random number generator for quadrat sampling from the potential locations identified by photogrammetry. Then a random distance up to 7 m from the center of the quadrat in any direction was generated to account for the size of each grid (15 m-by-15 m). A Garmin GPS (GPSMAP 67i Handheld GPS with inReach Satellite Technology, Garmin) was used to locate the location for quadrat sampling. The rope quadrat was laid down onto the site, and the quadrat was walked slowly in three passes ensuring that a thorough search for any stranded fish was completed. If a fish was stranded in the quadrat, the fish was kept in formalin for 24 h and then transferred to ethanol to identify to species and measure the total length (mm).

2.4 | Fish Community Sampling

Electrofishing was performed monthly on both rivers when the GS was peaking to determine fish species, life-stage, and density in the proximity of cameras. Five sites, each approximately 60 m^2 were randomly sampled each month at locations parallel to random camera locations during minimum discharge along the shoreline, as rivers are not fully wadable at maximum or minimum discharge. Locations were sampled using a direct current backpack electrofisher (LR-24 Backpack Electrofisher, Smith-Root Inc) with a maximum power output of 100 V, to a depth of about 60 cm, and at a pace of 4 $s\,m^{-2}$. A dip net with 3.2 mm mesh size and 304.8 mm bag depth was used to collect stunned fish. Captured fish were identified to species, age class (e.g., young-of-year, juvenile, and adult), counted, and returned to the river. A voucher specimen of unidentifiable fish species was kept for later identification in the lab using a microscope and a key (Scott and Crossman 1973). A cerebral percussion was performed to ensure euthanasia, then the fish was preserved in formalin for 24 h and then transferred into ethanol. Fish density (fish m^{-2}) was calculated at each electrofishing location during

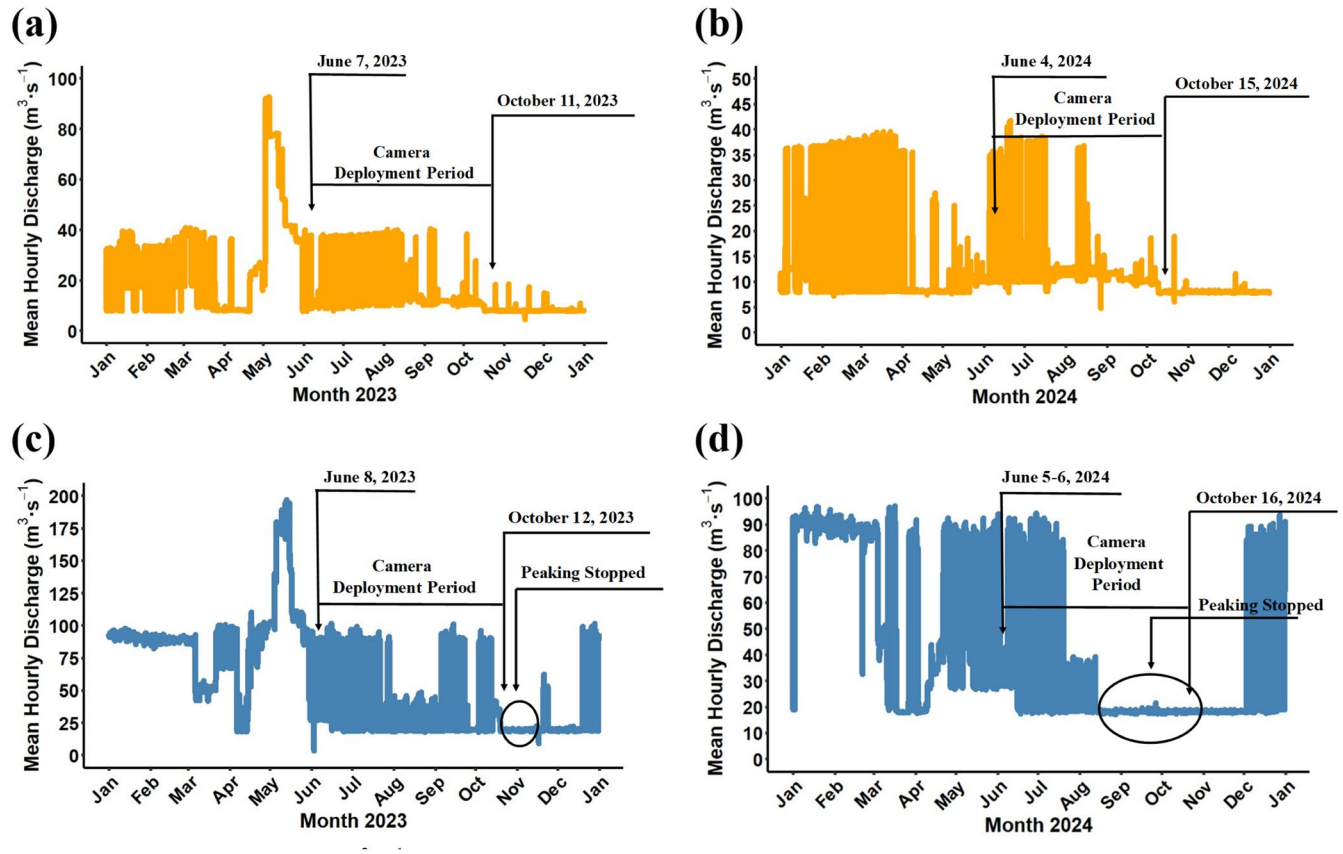

FIGURE 2 | Mean hourly discharge ($m^3 s^{-1}$) data (discharge data source), study period, and the camera deployment period are depicted for both rivers (a) Magpie River 2023 (Steephill Falls GS), (b) Magpie River 2024 (Steephill Falls GS), (c) Michipicoten River 2023 (Scott Falls GS), and (d) Michipicoten River 2024 (Scott Falls GS). [Color figure can be viewed at wileyonlinelibrary.com]

FIGURE 3 | Example of remotely deployed camera stands used to capture fish stranding occurrences on the Michipicoten and Magpie Rivers, Wawa, Ontario, Canada. [Color figure can be viewed at wileyonlinelibrary.com]

the study period and then assigned to each camera and quadrat by proximity to the electrofishing site and date closest to the observed peaking event.

2.5 | Habitat Classification

Habitat classification (e.g., substrate [mm], slope [%], and horizontal ramping rate [$cm\,h^{-1}$]) was assessed at each camera and quadrat location on both rivers.

Substrate assessments were performed using a photograph from each camera and quadrat location. The photographs of each location were brought into ImageJ (Schneider et al. 2012) and a 5-by-10 grid was overlayed on the photograph. Each cell was assigned a substrate size (mm, see Table S1 for substrate classification) based on the dominant substrate type (clay, silt, sand, gravel, pebble, cobble, and boulder) using a modified Wentworth Scale (Blair and McPherson 1999). The mean substrate size (mm) for each camera and quadrat location was determined by summing the grids and dividing by the total number of grids (50).

The mean slope (%) was collected at each camera and quadrat sampling location to calculate horizontal ramping rate ($cm\,h^{-1}$) and for comparison between rivers and locations of cameras and quadrats. To collect the mean slope (%), LiDAR data were collected using Polycam (Polycam Inc., 2021 Polycam, Los Angeles, CA, USA) on an iPad (iPad Pro version 16) at each camera and quadrat location. To capture the total area of each site (i.e., camera and quadrat sampling locations), the iPad was held at chest height and LiDAR was collected by walking the site in three passes (i.e., down the right side, up the middle, and down the left side). For processing in ArcGIS Pro v.3.1.0 (Redlands, CA,

USA), LAZ files were decompressed into LAS format in the lastools application (LAStools; rapidlasso GMbH, version 1.3.0). The LAS file was clipped to only include the sampled area for remote photography and quadrats using the built-in extract LAS function (Extract LAS 3D Analyst Tools) in ArcGIS Pro v. 3.1.0 (Redlands, CA, USA). To obtain the elevation (m) of the location the clipped LAS file was converted to a DEM using the built-in LAS dataset to Raster function in ArcGIS Pro v.3.1.0 (LAS Dataset to Raster Conversion Tools; Redlands, CA, USA). Finally, using the built-in slope function in ArcGIS Pro v.3.1.0 (Slope 3D Analyst Tools'; Redlands, CA, USA), the mean slope of the location was calculated using the created DEMs as a percent rise (%).

To determine vertical and horizontal ramping rates (cm h^{-1}) we deployed water level data loggers (Onset HOBO U20L-02 Water Level Data Logger, 100′, HOBO) that recorded water temperature and pressure at 30-min intervals. On the MR, six and eight level loggers were deployed in 2023 and 2024, respectively. On the MPR, six and five level loggers were deployed in 2023 and 2024, respectively. An additional logger was placed in a location that would remain dry to account for barometric correction of the water level data on both rivers in each year.

The vertical ramping rate (cm h^{-1}) was calculated for each observed peaking event at a camera by using the closest level logger, where d_{peak} represents the last water depth (cm) measurement at maximum discharge (e.g., the subsequent depth measurement must be ≥10 cm) and d_{dry} represents the depth (cm) when a camera was observed to be dry or the depth had stabilized at minimum discharge (e.g., changes in depth between subsequent measurements were ≤2 cm), and t represents the time (h) that the depth measurements were recorded, using the following equation:

$$\text{Vertical Ramping Rate}\left(\text{cm h}^{-1}\right) = \frac{d_{Dry} - d_{Peak}}{t_{Dry} - t_{Peak}}$$

The horizontal ramping rate (cm h^{-1}) was calculated for each observed peaking event at each camera location using the following equation:

$$\text{Horizontal Ramping Rate}\left(\text{cm h}^{-1}\right) = \frac{\text{Vertical Ramping Rate}\left(\text{cm h}^{-1}\right)}{\text{Mean Slope (\%)}} \times 100\%$$

2.6 | Image Analysis

Photographs were downloaded from the SD cards retrieved from the cameras during the monthly visits to the rivers. Each photograph from the cameras was manually inspected to identify the date and time that a site became wet—defined as when more than 50% of the photographed area was inundated with water, and dry—defined as when more than 50% of the photographed area had become dewatered after a peaking event (Figure 4). The time that a site remained wet (wetted history [min]) was calculated for each peaking event observed at a camera by subtracting the dry time from the wetted time. After each recorded peaking event for the cameras, the photographs leading up to and including when a site was completely dry were manually searched for stranded fish. All photographs were inspected by RD for consistency. If a fish was found, it was recorded, identified to species if possible, and total length (mm) was measured using ImageJ (Schneider et al. 2012).

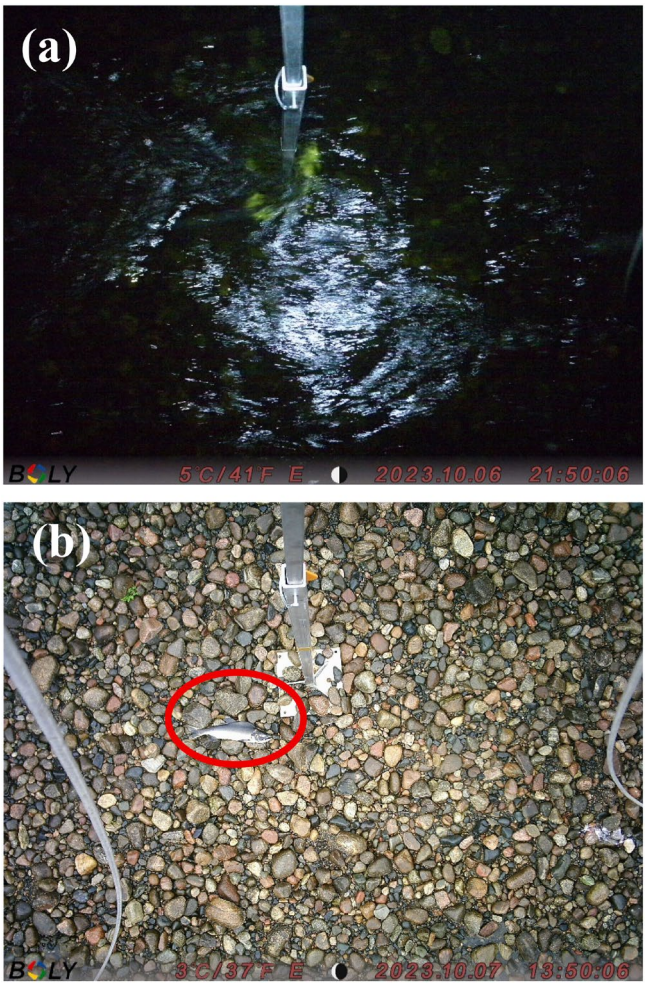

FIGURE 4 | (a) Photograph captured by remotely deployed camera demonstrating the location becoming inundated with water during the beginning of a peaking event. (b) Stranded fish is indicated by red circle. Fish was identified as a pink salmon (*Oncorhynchus gorbuscha*). [Color figure can be viewed at wileyonlinelibrary.com]

2.7 | Data and Statistical Analysis

Fish stranding density (fish m^{-2}) was calculated for each camera and quadrat for each peaking and sampling event, respectively, by dividing the total number of stranded fish at that camera or quadrat during that peaking or sampling event by the area of the photograph or quadrat. Fish stranding density did not meet the assumptions of normality and therefore Wilcoxon rank-sum tests were used for all comparisons in R v4.3.2 (R Core Team 2023) using the "base" R stats package (R Core Team 2023). To test for annual differences in fish stranding density on each river we compared: (1) densities between years for randomly deployed cameras; (2) densities between years for strategically deployed cameras; and (3) densities between years for quadrat sampling. Data were combined as no statistically significant differences were found between sampling years ($p > 0.05$). Fish stranding

densities captured by randomly and strategically deployed cameras were compared separately for each river to assess differences in camera deployment strategy. We then compared fish stranding densities between rivers for randomly and strategically deployed cameras to test for differences between rivers. A final test was performed to compare observed fish stranding density by sampling method, at random camera locations (filtered to only include peaking events on the same day as quadrat sampling) and quadrats.

A predictive model was only created for the MR due to the limited number of stranded fish observed on the MPR. To create the model, a binomial was created to denote fish stranding events occurring at a camera for each peaking event. If one or more fish were observed stranded at a camera during a peaking event, a score of 1 was assigned, and if no fish were observed stranded at a camera during a peaking event, a score of 0 was assigned. To determine if fish stranding events from both years and camera strategies (e.g., random and strategic) could be modeled together, a generalized linear model (GLM) using the "glm" function from the "base" stats package with a "logit link" function in R was used to develop a predictive model for the MR using year and camera strategy as predictors (R Core Team 2023).

Remote Photography Model 1

$$\begin{aligned} \textit{Fish Stranding Event} = \ & \textit{glm}(\textit{Fish Stranded} \sim \textit{Year} \\ & + \textit{Strategy}, \textit{family} = \textit{binomial}(\textit{link} = \textit{logit})) \end{aligned}$$

Subsequently, data collected from 2023 and 2024 could be modeled together but separate models were developed for randomly and strategically deployed cameras ($p < 0.001$). A generalized linear mixed-effects model using the "glmer" function from the "lme4" package (Bates et al. 2015) with a binomial distribution and "logit link" function was used to assess what predictors could be used to determine fish stranding probability. Predictive factors were scaled using a *Z*-score normalization and included electrofishing density (fish m^{-2}), wetted history (min), horizontal ramping rate (cm h^{-1}), calendar day (day), and substrate (mm). To account for repeated measurements at camera locations, camera site identification was used as a random effect. One random camera was removed in 2024 due to camera failures resulting in the inability to obtain data.

Remote Photography Model 2

$$\begin{aligned} \textit{Fish Stranding Event} = \ & \textit{glmer}(\textit{Fish Stranded} \sim \textit{Fish Density} \\ & + \textit{Wetted History} + \textit{Horizontal Ramping Rate} \\ & + \textit{Calendar Day} + \textit{Substrate} \\ & + (1|\ \textit{Camera ID}), \textit{family} = \textit{binomial}(\textit{link} = \textit{logit})) \end{aligned}$$

A GLM using the "glm" function from the base stats package with a logit link function was used to develop a predictive model for fish stranding occurrences at quadrat sampling locations (R Core Team 2023). Predictive factors were scaled using a *Z*-score normalization and included electrofishing density (fish m^{-2}), horizontal ramping rate (cm h^{-1}), calendar day (day), and substrate (mm).

Quadrat Model

$$\begin{aligned} \textit{Fish Stranding Event} = \ & \textit{glm}(\textit{Fish Stranded} \sim \textit{Fish Density} \\ & + \textit{Horizontal Ramping Rate} \\ & + \textit{Calendar Day} \\ & + \textit{Substrate}, \textit{family} = \textit{binomial}(\textit{link} = \textit{logit})) \end{aligned}$$

To determine if predictive factors known to influence fish stranding probability differed between rivers, a Principal Component Analysis (PCA) was performed. Using the "prcomp" function in R (R Core Team 2023). A PCA was performed to determine differences in the mean slope (%), substrate size (mm), and mean horizontal ramping rate (cm h^{-1}) for remote photography locations on both the MR and MPR. A PCA was conducted separately for random and strategic camera locations.

3 | Results

3.1 | Fish Stranding on the Michipicoten River

Remote photography and quadrats successfully captured fish stranding occurring downstream of Scott Falls GS on the MR (Table 1). In 2023, across all 11 cameras a total of 49 stranded fish were observed, with 11 fish observed stranded at random camera locations and 38 fish observed stranded at strategic camera locations. The maximum number of fish observed stranded at a single camera location during a peaking event was four. Most fish stranding events were observed at one strategic camera location, totaling 35 fish strandings over the 2023 study period. The fish stranding density was 0.004 ± 0.029 and 0.046 ± 0.120 fish m^{-2} at random and strategic camera locations, respectively. In 2023, quadrat sampling was completed in June and July only, and the observed fish stranding density was 0.013 ± 0.042 fish m^{-2} (Table 2).

In 2024, of the 33 cameras deployed, a total of 74 fish were observed stranded, with 17 fish stranded at random camera locations and 57 fish stranded at strategic camera locations. The maximum number of fish to strand at one camera location during one peaking event was eight. Two camera locations were responsible for a large number of fish strandings; these camera locations had 27 and 16 fish strand over the duration of the 2024 study period. The fish stranding density was 0.003 ± 0.020 and 0.020 ± 0.080 fish m^{-2} at random and strategic camera locations, respectively. In 2024, quadrats were sampled in June and July only, and the observed fish stranding density was 0.049 ± 0.141 fish m^{-2}.

3.2 | Fish Stranding Magpie River

Fish stranding was captured using remote photography on the MPR below Steephill Falls GS. Only one occurrence of fish stranding was observed using remote photography in both years, at a randomly and strategically deployed camera in 2023 and 2024, respectively. In 2023, the fish stranding density was 0 and 0.001 ± 0.129 fish m^{-2} at random and strategic camera locations, respectively. In 2024, the fish stranding density was 0.001 ± 0.009 and 0 ± 0 fish m^{-2} at random and strategic camera locations, respectively. Quadrat sampling was performed in

TABLE 1 | Mean ± SD of fish stranding density (fish m^{-2}) captured using remote photography for the Michipicoten and Magpie Rivers during camera deployment in 2023 and 2024.

River	Year	Strategy	Number of cameras	Total number of operational days	Total number of camera failure days	Total number of peaking events	Total area surveyed (m^2)	Total number of stranded fish	Total fish stranding density (fish m^{-2})
Michipicoten	2023	Random	8	981	27	362	2468.8	11	0.004 ± 0.029
Michipicoten	2023	Strategic	3	376	2	120	818.4	38	0.046 ± 0.120
Michipicoten	2024	Random	22	2857	339	763	5508.2	17	0.003 ± 0.020
Michipicoten	2024	Strategic	11	1077	123	283	2522.2	57	0.020 ± 0.080
Magpie	2023	Random	8	974	42	323	2188.3	0	0
Magpie	2023	Strategic	3	365	16	129	880.2	1	0.001 ± 0.129
Magpie	2024	Random	8	933	139	232	1716.6	1	0.000 ± 0.001
Magpie	2024	Strategic	3	376	26	141	962.1	0	0

TABLE 2 | Mean ± SD of fish stranding density (fish m^{-2}) obtained from quadrat sampling after a peaking event.

River	Year	Number of quadrats	Total area surveyed (m^2)	Number of stranded fish	Total fish stranding density (fish m^{-2})
Michipicoten	2023	23	149.5	2	0.013 ± 0.042
Michipicoten	2024	24	156	8	0.049 ± 0.001
Magpie	2023	24	156	0	0
Magpie	2024	12	156	0	0

Note: Data presented is for both 2023 and 2024.

June and July in 2023, and June only in 2024 where no fish were observed stranded in both years.

3.3 | Species Stranding Susceptibility

Electrofishing was performed on both rivers when their respective GS was operating with peaking events (see Tables S2 and S3 for summary of electrofishing results). Over both sampling years, 10 and 11 different species of fish were captured electrofishing, representing different life stages (e.g., young-of-year, juveniles, and adults) on the MR and MPR, respectively. Fish that were observed stranded using remote photography were challenging to identify, given similarities between species (e.g., chinook salmon, coho salmon, and rainbow trout). On the MR in 2023, using remote photography, we observed four adult pink salmon ($\overline{X}$ $TL = 368 \pm 19$ mm, $n = 4$), a young-of-year rainbow trout (28 mm), and eight sculpin species ($\overline{X}$ $TL = 55 \pm 13$ mm, $n = 8$). All other stranded fish were small-bodied with a mean total length of 27 ± 13 mm ($n = 36$). On the MR in 2024, using remote photography, we confidently identified two stranded fish as sculpin species ($\overline{X}$ $TL = 52 \pm 4$ mm, $n = 2$), and all other stranded fish were small-bodied with a mean total length of 30 ± 17 mm ($n = 72$). On the MPR in 2023, the stranded fish was identified as a northern pike (*Esox lucius*) with a total length of 74 mm and the stranded fish observed in 2024 was unidentifiable and could not be measured due to the position in the photographic frame. Quadrats allowed for the successful identification of stranded fish on the MR. In 2023, we observed one longnose dace (*Rhinichthys cataractae*) with a total length of 60 mm and an unmeasurable juvenile Pacific salmon species (e.g., coho salmon, chinook salmon, rainbow trout, or pink salmon). In 2024, we observed six young-of-year rainbow trout with a mean total length of 29 ± 1 mm and two juvenile Pacific salmon species (e.g., coho salmon, pink salmon, or chinook salmon) with a mean total length of 30 ± 0 mm.

3.4 | Comparison Between Strategies and Rivers

Using Wilcoxon rank-sum tests, no statistically significant differences in fish stranding density were found between years for either randomly (MR: $W = 138{,}666$, $p = 0.665$; MPR: $W = 37{,}307$, $p = 0.240$) or strategically deployed cameras (MR: $W = 17{,}682$, $p = 0.260$; MPR: $W = 9165$, $p = 0.299$) on each river. Similarly, fish stranding density did not differ between years for quadrat sampling on the MR ($W = 250$, $p = 0.349$). As a result, data from both years were combined for the subsequent comparisons.

Fish stranding density was significantly higher at strategically (0.030 ± 0.010 fish m^{-2}) than randomly (0.004 ± 0.025 fish m^{-2}) deployed cameras on the MR ($W = 202{,}496$, $p < 0.001$). On the MPR, fish stranding densities were similar between randomly (0.000 ± 0.006 fish m^{-2}) and strategically deployed cameras (0.000 ± 0.009 fish m^{-2}; $W = 74{,}783$, $p = 0.605$). Observed fish stranding density was significantly higher on the MR than the MPR for random ($W = 305{,}813$, $p = 0.001$) and strategic ($W = 47{,}585$, $p < 0.001$) cameras. Fish stranding density captured by randomly deployed cameras (0.008 ± 0.043 fish m^{-2}) was similar to quadrats (0.032 ± 0.106 fish m^{-2}) on the MR ($W = 1131.5$, $p = 0.096$).

3.5 | Fish Stranding Modeling

Model fitting of the data obtained from remote photography camera strategies resulted in a statistically significant difference between camera strategy ($p < 0.001$) but no difference between study years ($p = 0.369$). Model fitting of cameras that were placed at random camera locations demonstrated that day of the year was a statistically significant predictor of fish stranding probability ($p = 0.036$; Figure 5; Table S4). Fish stranding probability was highest earlier in the season with most fish stranding events occurring from June 14–July 14, 2023, and June 12–July 6, 2024. Model fitting of cameras that were placed at strategic camera locations demonstrated that slower horizontal ramping rates (cm h^{-1}; $p = 0.012$) and smaller substrate sizes (mm; $p = 0.007$) were statistically significant predictors of fish stranding probability (Figure 6; Table S5).

Model fitting of the data obtained from quadrat checks resulted in no statistically significant difference between study years ($p = 0.742$), and therefore both years were modeled together. A GLM revealed that no predictive factor had a statistically significant impact on fish stranding probability (Table S6).

3.6 | Comparison of River Habitats

PCA was used to explore the relationship between the habitat variables mean slope (%), substrate size (mm), and mean horizontal ramping rate (cm h^{-1}) at camera locations for both rivers (see Table S7 for summary of river characteristics). For randomly deployed cameras, the first two principal components explained 89.1% (PC1 = 61.6%, PC2 = 27.5%) of the variance observed between rivers (Figure 7a). Randomly deployed cameras on the MPR had larger substrate sizes (mm) and slower horizontal ramping rates (cm h^{-1}) than the MR. For strategically deployed cameras, the first two principal components explained 95.8% (PC1 = 54.7%, PC2 = 41.1%) of the variance observed between rivers (Figure 7b). Strategically deployed cameras on the MR had finer substrate sizes (mm) and faster horizontal ramping rates (cm h^{-1}) than the MPR. The mean slope (%) of the camera locations did not account for large amounts of variance between the two rivers for random or strategically deployed cameras, suggesting that the mean slopes (%) of the sites were comparable between the rivers at both camera strategies. Despite similar mean slopes (%) at camera locations, the mean vertical and horizontal ramping rates (cm h^{-1}) on the MR are much faster than the MPR (Figure 8).

4 | Discussion

In this study, we quantified fish stranding densities downstream of two hydroelectric generating stations using remote photography and quadrat sampling. Significantly higher observations of fish stranding were observed on the MR compared to the MPR for remote photography at both random and strategic camera locations. Stranded fish were difficult to identify to species using remote photography, although most fish were small-bodied, juvenile, and young-of-year fishes. Predictive models revealed that day of the year for randomly deployed cameras, and horizontal ramping rate (cm h^{-1}) and substrate (mm) for strategically deployed cameras were factors that significantly predicted fish stranding probability on the MR. Observed differences in fish stranding densities (fish m^{-2}) between the rivers are likely due to differences observed in horizontal ramping rates (cm h^{-1}) and substrate size (mm) at camera locations.

4.1 | Fish Stranding

Fish stranding densities differed between the two study rivers, with low observations of fish stranding on the MPR compared to the MR. Observed fish stranding densities on the MR were similar to those observed on the Saskatchewan River, Saskatchewan, Canada, where extrapolation resulted in upwards of one million fish stranding annually with average flow conditions (Glowa, Kneale, et al. 2023; Glowa, Watkinson, et al. 2023). It is unlikely that fish stranding on the MR is occurring at the same magnitude as the Saskatchewan River, Saskatchewan, Canada, due to differences in river size, species composition, and operational regimes. In the future, extrapolation of observed fish stranding density on each river could be used to explore annual fish stranding estimates using methods described by Glowa, Kneale, et al. (2023).

Fish stranding is known to be patchy and occur at locations with physical features, such as gentle slopes (Bradford et al. 1995; Führer et al. 2022; Hunter 1992), finer substrate types (Glowa, Watkinson, et al. 2023), and the presence of morphological microstructures (Insulaire et al. 2024; Irvine et al. 2015). Using this information, we deployed strategic cameras at sites thought to be conducive to fish stranding and we observed higher fish stranding densities (fish m^{-2}) at strategic cameras compared to randomly deployed cameras on the MR. Notable, is that 78 of 123 fish stranding events occurred at three strategic (out of 44 total) camera locations, demonstrating the patchiness of fish stranding. At these camera locations there were potholes which trapped fish during down-ramping, resulting in fish not being able to respond to changing flow conditions (Insulaire et al. 2024; Irvine et al. 2015).

Although transects are traditionally used to capture fish stranding occurrences (Dauwalter 2013; Glowa, Watkinson, et al. 2023; Irvine et al. 2015), here we deployed quadrats as it allowed for site specific data (e.g., slope [%], substrate size [mm]) to be quantified with the same precision as remote photography. Fish stranding densities were comparable between quadrats and remote photography, suggesting that quadrat sampling is a suitable method for capturing fish stranding on hydropeaking rivers.

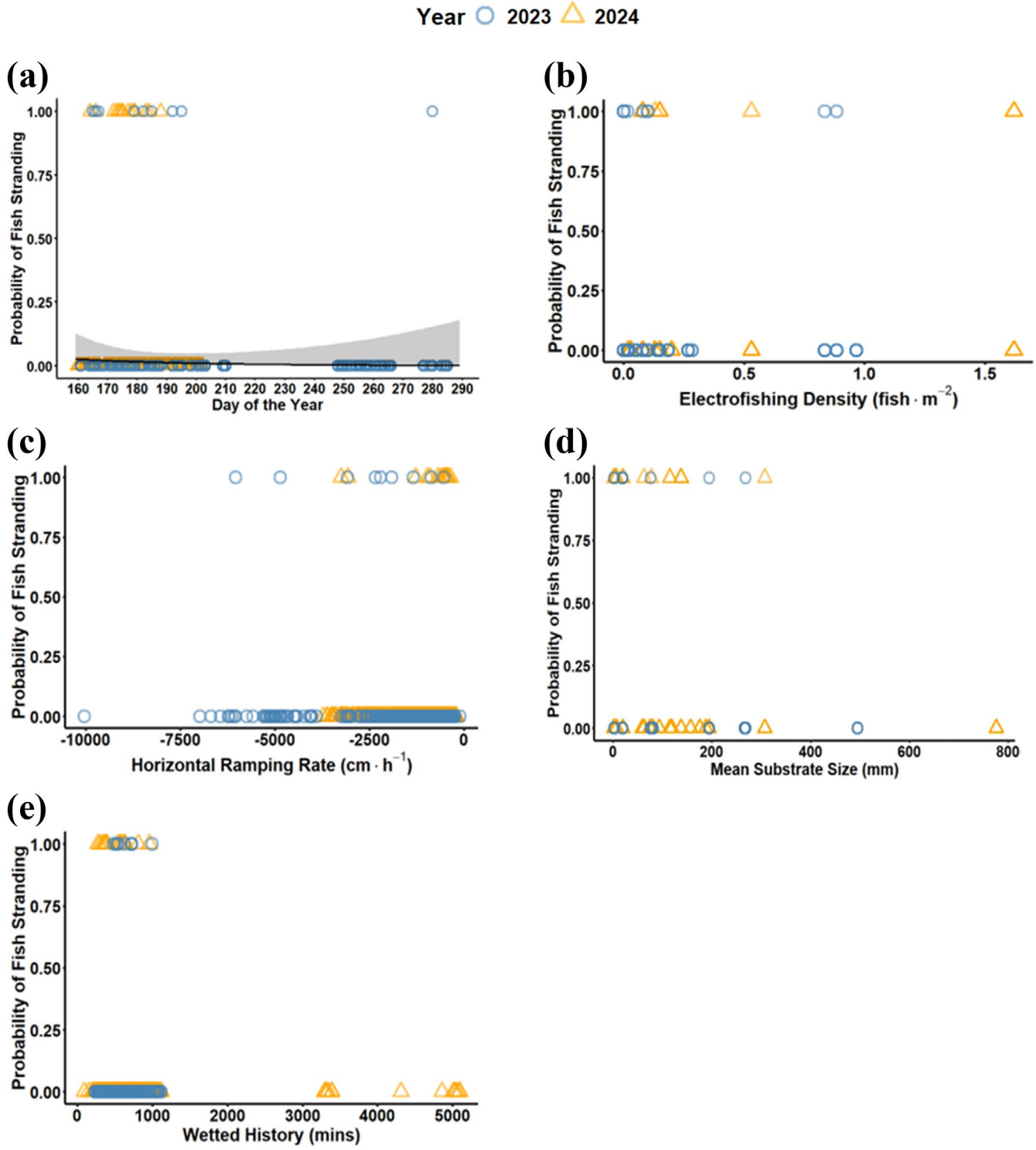

FIGURE 5 | Fit of the model for the response of fish stranding occurrence (0 = no fish stranded, 1 = fish stranded) observed from remote photography with cameras that were deployed at random camera locations with respect to the predictor variables (a) day of the year, (b) electrofishing density (fish m^{-2}), (c) horizontal ramping rate (cm h^{-1}), (d) mean substrate size (mm), and (e) wetted history. Each data point represents a peaking event observed at a camera location. Blue circles represent data from 2023 and orange triangles represent data from 2024. Variables with a significant relationship have a trendline to represent the relationship between variables. [Color figure can be viewed at wileyonlinelibrary.com]

4.2 | Fish Species and Body Size

Both rivers share similarity in the species present (e.g., sculpin species, white sucker [*Catostomus commersonii*], and longnose dace), with the biggest difference the presence of Pacific salmon on the MR (see Tables S2 and S3 for electrofishing summary). The inability to identify all stranded fish to species using remote photography makes it challenging to make conclusions about species stranding susceptibility. With the exception of the adult pink salmon, all fish that stranded were small-bodied,

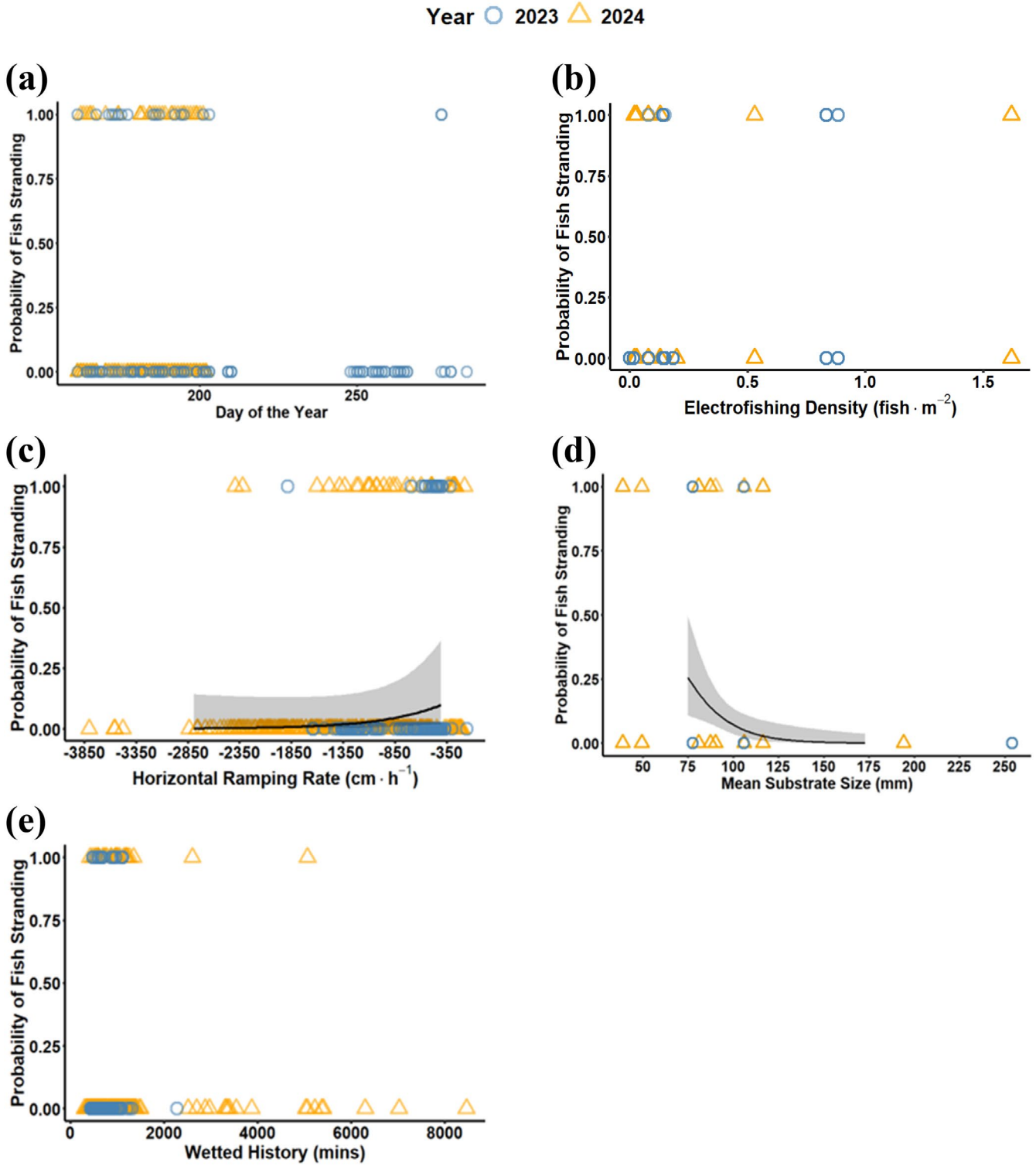

FIGURE 6 | Fit of the model for the response of fish stranding occurrence (0 = no fish stranded, 1 = fish stranded) observed from remote photography with cameras that were deployed at strategic camera locations with respect to the predictor variables (a) day of the year, (b) electrofishing density (fish m^{-2}), (c) horizontal ramping rate (cm h^{-1}), (d) mean substrate size (mm), and (e) wetted history (min). Each data point represents a peaking event observed at a camera location. Blue circles represent data from 2023 and orange triangles represent data from 2024. Variables with a significant relationship have a trendline to represent the relationship between variables. [Color figure can be viewed at wileyonlinelibrary.com]

likely representing juvenile and young-of-year fishes, similar to findings by others (Glowa, Watkinson, et al. 2023; Irvine et al. 2015; Nagrodski et al. 2012). The habitat preferences of these small fishes position them in areas of the river that become dewatered frequently, and their poor swimming capabilities increase their susceptibility to stranding during peaking events (Armstrong et al. 2003; Eppehimer et al. 2021; Haas et al. 2016; Insulaire et al. 2024; Irvine et al. 2015; Saltveit et al. 2001). The

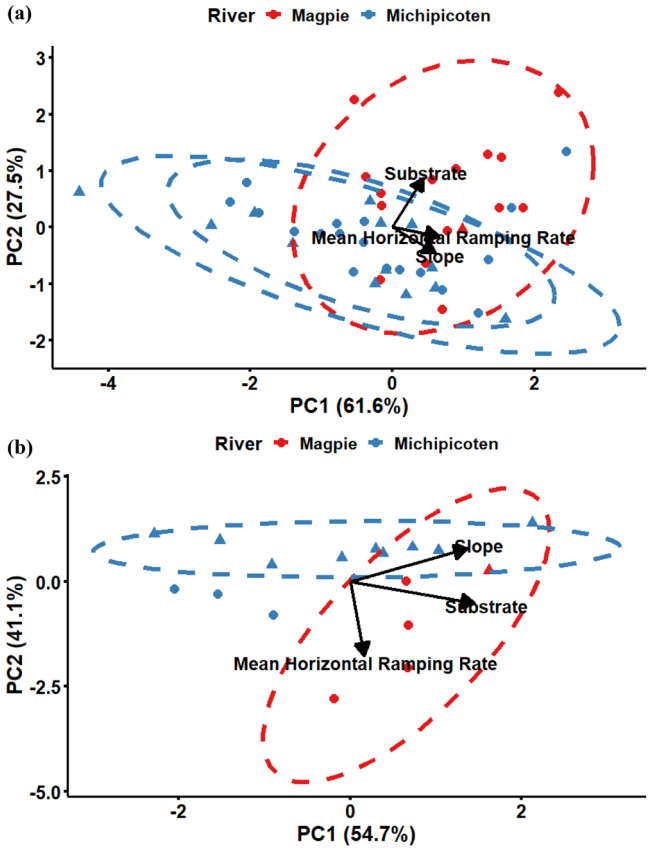

FIGURE 7 | Principal Component Analysis (PCA) projection showing the space defined by the (a) two first principal axes that explained 89.1% of the total variation for random camera locations and (b) two first principal axes that explained 95.8% of the total variation for strategic camera locations. Each data point corresponds to a strategically deployed camera location on the Magpie River shown in red and Michipicoten River shown in blue. Triangles represent camera locations where there was a fish stranding event during the study period and circles represent camera locations where no fish stranding occurred. The ellipses surround the centroid of each group representing a 95% confidence interval. [Color figure can be viewed at wileyonlinelibrary.com]

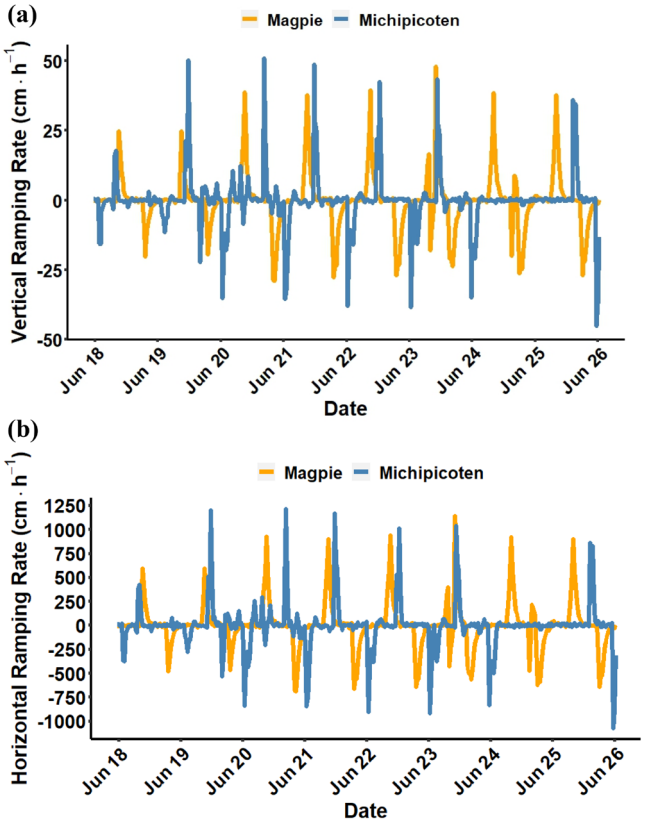

FIGURE 8 | (a) Example of mean vertical ramping rate (cm h^{-1}) (b) mean horizontal ramping rate (cm h^{-1}) obtained from water level loggers that were deployed below Scott Falls GS ($N = 6$) on the Michipicoten River, ON and Steephill Falls GS ($N = 5$) on the Magpie River, ON from June 18 to June 26, 2023. [Color figure can be viewed at wileyonlinelibrary.com]

stranding of the adult pink salmon may be a result of the lack of willingness for the female to leave her spawning redd at the onset of down-ramping but this is not highly documented in the literature (Nagrodski et al. 2012), although adult salmon are known to move into areas that become dewatered to create redds, increasing their susceptibility to stranding (Connor and Pflug 2004; Harnish et al. 2014; McMichael et al. 2005; Scott and Crossman 1973).

4.3 | Fish Stranding Predictive Modeling

At randomly deployed camera sites, we observed a negative relationship with fish stranding probability and calendar day. Fish stranding was most likely to occur from June to early July, which was also observed on the Columbia and Kootenay Rivers, British Columbia, Canada (Irvine et al. 2015) and may be due to a variety of factors. Peaking events on the MR were more frequent from June to early July than later in the season when peaking operations were restrained due to mitigative and operational constraints, which may be partially responsible for the increased probability of stranding early in the year. The high abundance of juvenile and young-of-year fishes, which are highly susceptible to stranding, may be contributing to a higher probability of stranding early in the summer (Armstrong et al. 2003; Glowa, Watkinson, et al. 2023; Haas et al. 2016; Irvine et al. 2015). In addition, fish stranding may decrease later in the season if the population becomes depleted due to mortality caused by peaking operations (Hayes et al. 2024) or as fish learn to avoid areas that become frequently dewatered during down-ramping (Capra et al. 2017; Judes et al. 2023). Notably, when Scott Falls GS was operating with an increased spring minimum of 26.3 m^3 s^{-1}, there were only three occurrences of fish stranding over both years suggesting that the increased minimum flow offers young-of-year and juvenile fishes protection from stranding.

At strategically deployed cameras, we observed a negative relationship with substrate size and fish stranding probability, as has been previously documented (Glowa, Watkinson, et al. 2023; Insulaire et al. 2024). Potholes are easily created on finer substrates due to the continual fluctuation of water, and these have been identified as stranding hotspots on other rivers (Auer et al. 2017; Insulaire et al. 2024). The strategic predictive model also demonstrated that slower horizontal ramping rates (cm h^{-1}) increased fish stranding probability; this finding is

not consistent with the literature as fish stranding typically increases with faster horizontal ramping rates (Irvine et al. 2015; Tuhtan et al. 2012). Horizontal ramping rate (cm h^{-1}) is slower with a steeper mean slope; the strategic camera sites that had high occurrences of fish stranding had potholes present, which artificially increased the mean slope of that site. At these camera locations, the surrounding river reach had gentle slopes (< 4%), suggesting that the overall reach had fast horizontal rates which would increase fish stranding probability (Hauer et al. 2017; Kopecki and Schneider 2016; Tuhtan et al. 2012). It is likely that fish using these areas avoided fast horizontal ramping rates by seeking refuge in potholes that remained wetted longer during down-ramping; however, as the potholes became dry the surrounding habitat (e.g., gravel bar) was already disconnected from the main river channel, resulting in the fish becoming stranded.

No relationship was observed between fish density (fish m^{-2}), horizontal ramping rate (cm h^{-1}), calendar day (day), substrate size (mm), and fish stranding probability at quadrat locations. This model lacks predictive power as we were only able to conduct quadrat sampling on 2 days during both study years. The lack of sampling is due to the GS not operating with a full peaking regime (e.g., fish could not strand because the discharge did not go from minimum flow to maximum flow and then back to minimum flow) during our monthly visits. In the future, it is recommended that more locations be sampled over multiple days each month when the GS is peaking to build a more robust model.

4.4 | Habitat and Operational Differences

The observed density of fish stranding was significantly higher on the MR in comparison to the MPR. PCA analysis of mean slope (%), substrate size (mm), and mean horizontal ramping rate (cm h^{-1}) at camera locations revealed that the habitat on the MR is more conducive to fish stranding than on the MPR, given the presence of faster horizontal ramping rates (cm h^{-1}) and finer substrate sizes (mm) on the MR (Auer et al. 2017; Glowa, Watkinson, et al. 2023; Insulaire et al. 2024). Although our model revealed that fish stranding increased with slower horizontal ramping rates at strategic camera locations on the MR, the literature suggests that fish stranding increases with faster horizontal ramping rates (Hauer et al. 2017; Kopecki and Schneider 2016; Tuhtan et al. 2012). The horizontal ramping rates are much slower on the MPR in comparison to the MR, suggesting that fish on the MPR have more time to respond to changes in flow conditions on the MPR than the MR. In addition, the larger substrate on the MPR may act to decrease the formation of morphological microstructures, which had high densities of fish stranding on the MR and other hydropeaking rivers globally (Auer et al. 2017; Insulaire et al. 2024).

The observed differences in mean horizontal ramping rate at camera locations between the two rivers cannot be explained by differences in the mean dam discharge down-ramping rate or the mean slope of camera locations. The mean dam discharge down-ramping rate ($m^3 s^{-1} min^{-1}$) is comparable between both rivers, so it is likely not responsible for the differences in observed horizontal ramping rates. Similarly, the mean slope (%) of camera locations does not differ greatly between the rivers, with both rivers generally having gentle slopes (≤ 4%). Therefore, the mean slope (%) of sites is likely not responsible for the large difference in observed horizontal ramping rate. We suggest that the presence of a large plunge pool at the base of the dam on the MPR dampens the change in discharge from the GS, resulting in slower vertical ramping rates (cm h^{-1}) downstream from the GS, which translates to slower horizontal ramping rates (cm h^{-1}). In fact, basins and caverns have been constructed below dams specifically as a structural mitigation to dampen ramping rates (Premstaller et al. 2017; Tonolla et al. 2017). The observed differences in vertical and horizontal ramping rates provide fish with more time to respond to fluctuations in flow changes on the MPR compared to the MR. Although there are physical differences between the rivers (e.g., larger substrates, lack of potholes) and fish species differences (e.g., pink salmon, chinook salmon, coho salmon, and rainbow trout), we suggest that the plunge pool is highly responsible for mitigating fish stranding on the MPR.

4.5 | Benefits and Limitations of Remote Photography

Remote photography, quadrats, and transects are all methods that have been used to investigate fish stranding, and tradeoffs exist for each method. Remote photography provides broad temporal data which could not be accomplished with other sampling methods due to the inability and feasibility for field staff to conduct transect surveys weekly on the river. Capturing of photographs every 30 min allows for predictive factors such as wetted history (min) and ramping rates (e.g., vertical and horizontal ramping rates; cm h^{-1}) to be quantified more precisely than other sampling methods. Although temporal coverage is increased, there is a decrease in spatial coverage with remote photography. In 2024, on the MR, on a single day when all cameras were working, only 255 m^2 of river area was sampled. To contrast, transect surveys conducted in 1 day on the South Fork Boise River covered approximately 25.8 km^2 of river area (assuming viewer visibility is 3 m and 8.6 km of linear shoreline was surveyed; Dauwalter 2013). The large increase in spatial coverage when comparing transects to remote photography might result in an increase in fish stranding densities because there is a higher likelihood of encountering a patch of stranded fish (Glowa, Watkinson, et al. 2023), but the large temporal coverage exhibited from remote photography methodology is lost. Other limitations of remote photography include camera failures, difficulty identifying stranded fish to species, and challenges observing fish on large substrate types (e.g., cobble and boulder) where fish can be hidden in the interstitial spaces.

In the future, we suggest that a combination of methods be employed to investigate factors that influence fish stranding. For example, if camera stands are deployed, transects could be sampled weekly and quadrats could be employed alongside transects when fish are found stranded (e.g., quadrat is centered around the stranded fish), and habitat data could be collected. This combination of methods could increase temporal and spatial coverage while also providing information on species identification, which was a challenge using remote photography.

4.6 | Mitigation of Fish Stranding

Structural and operational mitigation measures could be used to decrease fish stranding occurrences on the MR. On the MR, structural mitigation measures that could be considered to reduce fish stranding include the construction of basins or caverns (see Premstaller et al. 2017; Tonolla et al. 2017) and the recontouring of the substrate to reduce morphological microstructures (e.g., potholes) where fish stranding occurred frequently (Irvine et al. 2015). Operational mitigation measures could also be used to reduce fish stranding occurrences on the MR. On the MR, operational mitigation measures that could be considered to reduce fish stranding include a maximum dam down-ramping rate during spring to protect juvenile and young-of-year fishes (Le Coarer et al. 2023; Moreira et al. 2019) and a reduction of peaking operations during critical times of the year, such as spawning (Connor and Pflug 2004; Harnish et al. 2014; McMichael et al. 2005). As of now, the operators on the MR have eliminated peaking operations during the Pacific salmon spawning season and will perform manual salvage efforts to return any stranded fish back to the main river channel if any peaking occurs (see Figure 2c,d for the annual hydrograph of the MR).

With the increasing development of hydropower projects globally, we recommend that the MPR be used as a design example (Zarfl et al. 2015). The plunge pool located below Steephill Falls GS likely dampens the change in discharge, which translates to lower vertical and horizontal ramping rates ($cm\,h^{-1}$). Although creating a plunge pool below current hydropeaking generating stations would be costly and disrupt the river habitat, it could be implemented to mitigate fish stranding. Furthermore, we suggest that plunge pools be considered as a mitigation strategy during the construction of new facilities, highlighting the importance of strategic planning in future developments to help protect fish from stranding (Almeida et al. 2022).

In conclusion, our study determined that fish stranding density ($fish\,m^{-2}$) differed significantly between study rivers with minimal occurrences of fish stranding on the MPR compared to the MR. Fish stranding density ($fish\,m^{-2}$) was different between camera strategies (e.g., random vs. strategic) but not methodology (e.g., quadrats vs. remote photography), suggesting a combination of sampling techniques (e.g., remote photography, quadrats, and transects) could be used to determine fish stranding density ($fish\,m^{-2}$). Predictive modeling determined that fish stranding was more likely to occur early in the year at random camera locations, and on finer substrates (mm) with slower horizontal ramping rates ($cm\,h^{-1}$) at strategic camera locations, which is similar to other rivers (Le Coarer et al. 2023; Glowa, Watkinson, et al. 2023; Irvine et al. 2015). Observed differences in fish stranding between the study rivers is likely a combination of differences in mean slope (%), substrate size (mm), and mean horizontal ramping rate ($cm\,h^{-1}$) of camera locations on both rivers. Although the generating stations have similar dam down-ramping rates ($m^3\,s^{-1}\,min^{-1}$), the observed vertical and horizontal ramping rates ($cm\,h^{-1}$) at cameras are much faster on the MR, suggesting that the natural plunge pool dampens the changes in discharge from the GS. Potentially, the design and physical features of the MPR could provide insights to guide future developments towards rivers and features that may be suitable, allowing fish to be protected while energy demands are met.

Acknowledgments

This study was financially supported by Evolugen (a Brookfield Renewable company), Fisheries and Oceans Canada, Carleton University, and the Natural Sciences and Engineering Research Council of Canada. We thank Evan Timusk, Rick Elsner, and Sarah Glowa for their support in conducting field work and data collection. We also thank Douglas Watkinson for his development of the photography methodology and for providing us with the equipment necessary to complete this project.

Funding

This work was supported by Evolugen by Brookfield Power; Fisheries and Oceans Canada; Carleton University; Natural Sciences and Engineering Research Council of Canada.

Conflicts of Interest

The authors declare no conflicts of interest.

Data Availability Statement

The data that support the findings of this study are available from the corresponding author upon reasonable request.

References

Almeida, R. M., R. J. Schmitt, A. Castelletti, et al. 2022. "Strategic Planning of Hydropower Development: Balancing Benefits and Socioenvironmental Costs." *Current Opinion in Environmental Sustainability* 56: 101175. https://doi.org/10.1016/j.cosust.2022.101175.

Armstrong, J. D., P. S. Kemp, G. J. A. Kennedy, M. Ladle, and N. J. Milner. 2003. "Habitat Requirements of Atlantic Salmon and Brown Trout in Rivers and Streams." *Fisheries Research* 62, no. 2: 143–170. https://doi.org/10.1016/S0165-7836(02)00160-1.

Auer, S., B. Zeiringer, S. Führer, D. Tonolla, and S. Schmutz. 2017. "Effects of River Bank Heterogeneity and Time of Day on Drift and Stranding of Juvenile European Grayling (*Thymallus thymallus* L.) Caused by Hydropeaking." *Science of the Total Environment* 575: 1515–1521. https://doi.org/10.1016/j.scitotenv.2016.10.029.

Bates, D., M. Maechler, B. Bolker, and S. Walker. 2015. "Fitting Linear Mixed-Effects Models Using lme4." *Journal of Statistical Software* 67, no. 1: 1–48. https://doi.org/10.18637//jss.v067.i01.

Batson, D. 2021. "Exactextractr: Fast Extraction From Raster Datasets Using Polygons." R Package Version 0.7.2. https://CRAN.R-project.org/package=exactextractr.

Bauer, N., K. Calvin, J. Emmerling, et al. 2017. "Shared Socio-Economic Pathways of the Energy Sector—Quantifying the Narratives." *Global Environmental Change* 42: 316–330. https://doi.org/10.1016/j.gloenvcha.2016.07.006.

Béjar, M., D. Vericat, R. J. Batalla, and C. N. Gibbins. 2018. "Variation in Flow and Suspended Sediment Transport in a Montane River Affected by Hydropeaking and Instream Mining." *Geomorphology (Amsterdam, Netherlands)* 310: 69–83. https://doi.org/10.1016/j.geomorph.2018.03.001.

Bejarano, M. D., R. Jansson, and C. Nilsson. 2018. "The Effects of Hydropeaking on Riverine Plants: A Review." *Biological Reviews of the Cambridge Philosophical Society* 93, no. 1: 658–673. https://doi.org/10.1111/brv.12362.

Berga, L. 2016. "The Role of Hydropower in Climate Change Mitigation and Adaptation: A Review." *Engineering* 2, no. 3: 313–318. https://doi.org/10.1016/J.ENG.2016.03.004.

Bivand, R., T. Keitt, and B. Rowlingson. 2021. "RGDAL: Bindings for the 'Geospatial' Data Abstraction Library." R Package Version 1.5-27. https://CRAN.R-project.org/package=rgdal.

Bivand, R., and C. Rundel. 2021. "Rgeos: Interface to Geometry Engine-Open Source ('GEOS')." R Package Version 0.5-8. https://CRAN.R-project.org/package=rgeos.

Blair, T. C., and J. G. McPherson. 1999. "Grain-Size and Textural Classification of Coarse Sedimentary Particles." *Journal of Sedimentary Research* 69, no. 1: 6–19. https://doi.org/10.2110/jsr.69.6.

Bradford, M. J. 1997. "An Experimental Study of Stranding of Juvenile Salmonids on Gravel Bars and in Sidechannels During Rapid Flow Decreases." *Regulated Rivers: Research & Management* 13, no. 5: 395–401. https://doi.org/10.1002/(SICI)1099-1646(199709/10)13:5<395::AID-RRR464>3.0.CO;2-L.

Bradford, M. J., G. C. Taylor, J. A. Allan, and P. S. Higgins. 1995. "An Experimental Study of the Stranding of Juvenile Coho Salmon and Rainbow Trout During Rapid Flow Decreases Under Winter Conditions." *North American Journal of Fisheries Management* 15, no. 2: 473–479. https://doi.org/10.1577/1548-8675(1995)015<0473:AESOTS>2.3.CO;2.

Butterfield, B. J., and E. C. Palmquist. 2025. "Daily Fluctuating Flows Affect Riparian Plant Species Distributions From Local to Regional Scales." *Applied Vegetation Science* 28, no. 3: 1–14. https://doi.org/10.1111/avsc.70033.

Capra, H., L. Plichard, J. Bergé, et al. 2017. "Fish Habitat Selection in a Large Hydropeaking River: Strong Individual and Temporal Variations Revealed by Telemetry." *Science of the Total Environment* 578: 109–120. https://doi.org/10.1016/j.scitotenv.2016.10.155.

Connor, E. J., and D. E. Pflug. 2004. "Changes in the Distribution and Density of Pink, Chum, and Chinook Salmon Spawning in the Upper Skagit River in Response to Flow Management Measures." *North American Journal of Fisheries Management* 24, no. 3: 835–852. https://doi.org/10.1577/M03-066.1.

Dauwalter, D. 2013. "A Pilot Study of Fish Stranding on the South Fork Boise River, 2012." https://southforkboise.org/wp-content/uploads/2013/07/2012SFBoise_StrandingSummary.pdf.

Enders, E. C., D. A. Watkinson, H. Ghamry, K. H. Mills, and W. G. Franzin. 2017. "Fish Age and Size Distributions and Species Composition in a Large, Hydropeaking Prairie River." *River Research and Applications* 33, no. 8: 1246–1256. https://doi.org/10.1002/rra.3173.

Eppehimer, D. E., B. J. Enger, A. E. Ebenal, E. P. Rocha, and M. T. Bogan. 2021. "Daily Flow Intermittence in an Effluent-Dependent River: Impacts of Flow Duration and Recession Rate on Fish Stranding." *River Research and Applications* 37, no. 10: 1376–1385. https://doi.org/10.1002/rra.3850.

Führer, S., D. S. Hayes, T. Hasler, et al. 2022. "Stranding of Larval Nase (*Chondrostoma nasus* L.) Depending on Bank Slope, Down-Ramping Rate and Daytime." *Frontiers in Environmental Science* 10, no. 966418: 1–18. https://doi.org/10.3389/fenvs.2022.966418.

Glowa, S. E., A. J. Kneale, D. A. Watkinson, H. K. Ghamry, E. C. Enders, and T. D. Jardine. 2023. "Applying a Two-Dimensional Hydrodynamic Model to Estimate Fish Stranding Risk Downstream From a Hydropeaking Hydroelectric Station." *Ecohydrology* 16, no. 4: 1–15. https://doi.org/10.1002/eco.2530.

Glowa, S. E., D. A. Watkinson, T. D. Jardine, and E. C. Enders. 2023. "Evaluating the Risk of Fish Stranding due to Hydropeaking in a Large Continental River." *River Research and Applications* 39, no. 3: 444–459. https://doi.org/10.1002/rra.4083.

Haas, C., P. Zinke, K. W. Vollset, J. Sauterleute, and H. Skoglund. 2016. "Behaviour of Spawning Atlantic Salmon and Brown Trout During Ramping Events." *Journal of Applied Water Engineering and Research* 4, no. 1: 25–30. https://doi.org/10.1080/23249676.2016.1169227.

Harnish, R. A., R. Sharma, G. A. McMichael, R. B. Langshaw, and T. N. Pearsons. 2014. "Effect of Hydroelectric Dam Operations on the Freshwater Productivity of a Columbia River Fall Chinook Salmon Population." *Canadian Journal of Fisheries and Aquatic Sciences* 71, no. 4: 602–615. https://doi.org/10.1139/cjfas-2013-0276.

Hauer, C., P. Holzapfel, P. Leitner, and W. Graf. 2017. "Longitudinal Assessment of Hydropeaking Impacts on Various Scales for an Improved Process Understanding and the Design of Mitigation Measures." *Science of the Total Environment* 575: 1503–1514. https://doi.org/10.1016/j.scitotenv.2016.10.031.

Hayes, D. S., S. Auer, E. Fauchery, et al. 2023. "The Interactive Effect of River Bank Morphology and Daytime on Downstream Displacement and Stranding of Cyprinid Larvae in Hydropeaking Conditions." *Ecohydrology & Hydrobiology* 23, no. 1: 152–161. https://doi.org/10.1016/j.ecohyd.2022.12.001.

Hayes, D. S., N. Bätz, D. Tonolla, et al. 2024. "Why Hydropeaking Frequency Matters: Effects of Recurring Stranding on Fish." *Journal of Ecohydraulics* 10, no. 3: 1–17. https://doi.org/10.1080/24705357.2024.2426820.

Hunter, M. A. 1992. *Hydropower Flow Fluctuations and Salmonids: A Review of the Biological Effects, Mechanical Causes, and Options for Mitigation (Tech. Rep. 119)*. State of Washington, Department of Fisheries, Habitat Management Division.

Insulaire, F., N. Lamouroux, A. Barillier, et al. 2024. "Characterizing the Effects of Morphological Microstructures and Hydropeaks on Fish Stranding in Rivers." *River Research and Applications* 40, no. 5: 834–849. https://doi.org/10.1002/rra.4277.

Intergovernmental Panel on Climate Change (IPCC). 2023. "Terrestrial and Freshwater Ecosystems and Their Services." In *Climate Change 2022—Impacts, Adaptation and Vulnerability: Working Group II Contribution to the Sixth Assessment Report of the Intergovernmental Panel on Climate Change*, 197–378. Cambridge University Press.

Irvine, R. L., J. L. Thorley, R. Westcott, D. Schmidt, and D. DeRosa. 2015. "Why Do Fish Strand? An Analysis of Ten Years of Flow Reduction Monitoring Data From the Columbia and Kootenay Rivers, Canada." *River Research and Applications* 31, no. 10: 1242–1250. https://doi.org/10.1002/rra.2823.

Judes, C., H. Capra, V. Gouraud, et al. 2023. "Past Hydraulics Influence Microhabitat Selection by Invertebrates and Fish in Hydropeaking Rivers." *River Research and Applications* 39, no. 3: 375–388. https://doi.org/10.1002/rra.3981.

Kjærstad, G., J. V. Arnekleiv, J. D. M. Speed, et al. 2018. "Effects of Hydropeaking on Benthic Invertebrate Community Composition in Two Central Norwegian Rivers." *River Research and Applications* 34, no. 3: 218–231. https://doi.org/10.1002/rra.3241.

Kopecki, I., and M. Schneider. 2016. "Operational and Structural Measures to Reduce Hydropeaking Impact on Fish Larvae." *La Houille Blanche* 102, no. 6: 48–53. https://doi.org/10.1051/lhb/2016060.

Larrieu, K. G., G. B. Pasternack, and S. Schwindt. 2021. "Automated Analysis of Lateral River Connectivity and Fish Stranding Risks—Part 1: Review, Theory and Algorithm." *Ecohydrology* 14, no. 2: 1–11. https://doi.org/10.1002/eco.2268.

Le Coarer, Y., M. Lizée, L. Beche, and M. Logez. 2023. "Horizontal Ramping Rate Framework to Quantify Hydropeaking Stranding Risk for Fish." *River Research and Applications* 39, no. 3: 478–489. https://doi.org/10.1002/rra.4087.

Li, T., and G. B. Pasternack. 2021. "Revealing the Diversity of Hydropeaking Flow Regimes." *Journal of Hydrology (Amsterdam)* 598: 126392. https://doi.org/10.1016/j.jhydrol.2021.126392.

McMichael, G. A., C. A. McKinstry, J. A. Vucelick, and J. A. Lukas. 2005. "Fall Chinook Salmon Spawning Activity Versus Daylight and Flow in the Tailrace of a Large Hydroelectric Dam." *North American Journal of Fisheries Management* 25, no. 2: 573–580. https://doi.org/10.1577/M04-044.1.

Moreira, M., D. S. Hayes, I. Boavida, M. Schletterer, S. Schmutz, and A. Pinheiro. 2019. "Ecologically-Based Criteria for Hydropeaking Mitigation: A Review." *Science of the Total Environment* 657: 1508–1522. https://doi.org/10.1016/j.scitotenv.2018.12.107.

Nagrodski, A., G. D. Raby, C. T. Hasler, M. K. Taylor, and S. J. Cooke. 2012. "Fish Stranding in Freshwater Systems: Sources, Consequences, and Mitigation." *Journal of Environmental Management* 103: 133–141. https://doi.org/10.1016/j.jenvman.2012.03.007.

Nguyen, B. Q., S. A. Kantoush, T.-N.-D. Tran, T. H. Nguyen, T. Sumi, and S. Kobayashi. 2025. "Long-Term Assessment of Hydropeaking and Cumulative Impacts on Sediment Transport, Grain Size Dynamics, Channel Stability and Water Resource Management." *Journal of Environmental Management* 380: 124983. https://doi.org/10.1016/j.jenvman.2025.124983.

Premstaller, G., V. Cavedon, G. R. Pisaturo, S. Schweizer, V. Adami, and M. Righetti. 2017. "Hydropeaking Mitigation Project on a Multi-Purpose Hydro-Scheme on Valsura River in South Tyrol/Italy." *Science of the Total Environment* 574: 642–653. https://doi.org/10.1016/j.scitotenv.2016.09.088.

R Core Team. 2023. *R: A Language and Environment for Statistical Computing*_. R Foundation for Statistical Computing. https://www.R-project.org/.

Saltveit, S. J., J. H. Halleraker, J. V. Arnekleiv, A. Harby, and S. Lane. 2001. "Field Experiments on Stranding in Juvenile Atlantic Salmon (*Salmo salar*) and Brown Trout (*Salmo trutta*) During Rapid Flow Decreases Caused by Hydropeaking." *Regulated Rivers Research & Management* 17: 609–622.

Schneider, C. A., W. S. Rasband, and K. W. Eliceiri. 2012. "NIH Image to ImageJ: 25 Years of Image Analysis." *Nature Methods* 9, no. 7: 671–675.

Scott, W. B., and E. J. Crossman. 1973. *Freshwater Fishes of Canada*. Fisheries Research Board of Canada.

Smokorowski, K. E. 2022. "The Ups and Downs of Hydropeaking: A Canadian Perspective on the Need for, and Ecological Costs of, Peaking Hydropower Production." *Hydrobiologia* 849, no. 2: 421–441. https://doi.org/10.1007/s10750-020-04480-y.

Timusk, E. R., K. E. Smokorowski, and N. E. Jones. 2016. "An Experimental Test of Sub-Hourly Changes in Macroinvertebrate Drift Density Associated With Hydropeaking in a Regulated River." *Journal of Freshwater Ecology* 31, no. 4: 555–570. https://doi.org/10.1080/02705060.2016.1193064.

Tonolla, D., A. Bruder, and S. Schweizer. 2017. "Evaluation of Mitigation Measures to Reduce Hydropeaking Impacts on River Ecosystems—A Case Study From the Swiss Alps." *Science of the Total Environment* 574: 594–604. https://doi.org/10.1016/j.scitotenv.2016.09.101.

Tuhtan, J. A., M. Noack, and S. Wieprecht. 2012. "Estimating Stranding Risk due to Hydropeaking for Juvenile European Grayling Considering River Morphology." *KSCE Journal of Civil Engineering* 16, no. 2: 197–206. https://doi.org/10.1007/s12205-012-0002-5.

Young, P. S., J. J. Cech, and L. C. Thompson. 2011. "Hydropower-Related Pulsed-Flow Impacts on Stream Fishes: A Brief Review, Conceptual Model, Knowledge Gaps, and Research Needs." *Reviews in Fish Biology and Fisheries* 21, no. 4: 713–731. https://doi.org/10.1007/s11160-011-9211-0.

Zarfl, C., A. E. Lumsdon, J. Berlekamp, L. Tydecks, and K. Tockner. 2015. "A Global Boom in Hydropower Dam Construction." *Aquatic Sciences* 77, no. 1: 161–170. https://doi.org/10.1007/s00027-014-0377-0.

Supporting Information

Additional supporting information can be found online in the Supporting Information section. **Table S1:** rra70113-sup-0001-TableS1-S7.docx.